Phys Chem Minerals (2004) 31: 195–202
DOI 10.1007/s00269-003-0361-z

ORIGINAL PAPER

M. D. Alba · M. A. Castro · M. Naranjo
A. C. Perdigón

Structural localization of Al^{3+} ions in aluminosilicates: application of heteronuclear chemical shift correlation to 2:1 phyllosilicates

Received: 19 May 2003 / Accepted: 25 August 2003

Abstract The main objective of this paper is to apply an NMR-based methodology to clay minerals that provides resolution enhancement in ^{27}Al NMR spectra, permitting the differentiation of aluminum ions with one same coordination number, but with different chemical environments. For this purpose, we have performed two-dimensional $^{1}H \rightarrow ^{27}Al$ cross-polarization experiments, which facilitate the identification of the different aluminum crystallographic sites by means of the nature of the proton polarization source. For the development of this methodology, we have carried out a systematic study of a set of well-characterized 2:1 phyllosilicates with aluminum in different crystallographic sites. The structural locations of aluminum in the selected layered silicates have been established unequivocally. Once the correlation between all different aluminum and proton sites in smectite was well established, an unknown material was examined, the utility of this methodology being illustrated. This methodology can be applied to a great variety of materials, such as zeolites, ALPOs and mesoporous aluminosilicates, in which a precise determination of the aluminum location is demanded.

Keywords ^{27}Al NMR spectra · Aluminum ions · Cross-polarization

Introduction

Over the past decades considerable efforts have been devoted to developing silicates with applications in heterogeneous acidic catalysis (Weisz and Frilette 1960; Figueras et al. 1988; Mitchell el al. 1990; Mokaya et al. 1996). The catalytic properties of these materials rely on the presence of active (e.g. acidic) sites in their framework. The active sites may be generated by the incorporation of heteroatoms into the siliceous framework, the incorporation of aluminum being particularly important as it gives rise to Brönsted acid sites. There are well-known difficulties encountered in evaluating the amount of aluminum incorporated into the framework during the synthesis of aluminosilicates (Ray et al. 1987) and in estimating the aluminum leaching during the thermal and hydrothermal treatments of these solids (Yingcai et al. 1996). A promising technique to study the chemical environment of aluminum in crystalline and amorphous solids is solid-state nuclear magnetic resonance.

Since 1979 there has been a growing use of high-resolution magic-angle-spinning nuclear magnetic resonance (MAS NMR) spectroscopy to study minerals (Kirkpatrick et al. 1985; Oldfield and Kirkpatrick 1985). The study of quadrupolar nuclei such as ^{27}Al was initially avoided because the quadrupolar interaction produces broad featureless peaks for powdered samples. In the early 1980s, high-resolution ^{27}Al MAS NMR spectra were obtained under conditions of magic-angle spinning, high magnetic field strengths and only $(+1/2 \rightarrow -1/2)$ spin transition observation (Meadows et al. 1982).

Although MAS NMR is used routinely to average anisotropy interactions, a single-pulse sequence is not always the most appropriate choice in these systems in terms of extracting structural information regarding the coordination number and geometry, the nature of the attached atoms, etc. from ^{27}Al MAS NMR spectra. Muller et al. (1981) found that little structural information could be obtained for aluminates and aluminosilicates from low-field ^{27}Al spectra dominated by quadrupolar interactions. Whereas the coordination number of the AlO_n polyhedra can be determined unambiguously, even from relatively broad lines and uncorrected chemical shift data, the identification of different aluminum environments with the same coordination number is more difficult because the ^{27}Al

M. D. Alba (✉) · M. A. Castro · M. Naranjo · A. C. Perdigón
Instituto de Ciencia de Materiales de Sevilla,
Departamento de Química Inorgánica,
Consejo Superior de Investigaciones Científicas-Universidad de Sevilla,
Avda. Américo Vespucio s/n. 41092-Sevilla, Spain
e-mail: alba@icmse.csic.es

chemical shifts are not very sensitive to the chemical environment. These difficulties can be overcome with a technique such as cross-polarization combined with MAS (CPMAS), which increases the available information of the spectra because it provides additional information related to spatial proximity between proton and aluminum nuclei. Moreover, two-dimensional $^{1}H \rightarrow X$ cross-polarization experiments allow the establishment of spatial correlation between the proton and the observed nuclei. The success of CPMAS in the identification of signals from crystallographically inequivalent spin-1/2 nuclei in solids is widely proved and $^{1}H \rightarrow ^{29}Si$ and $^{1}H \rightarrow ^{13}C$ spatial correlations have been observed. However, some difficulties in applying it to quadrupolar nuclei were found (Vega 1992; Blumenfeld and Fripiat 1997), due to the fact that the Hartmann-Hahn relationship is rigorously valid only for nuclei without any quadrupolar interaction.

In order to perform two-dimensional $^{1}H \rightarrow ^{27}Al$ cross-polarization experiments, two difficulties need to be overcome. First, special care needs to be taken to transfer polarization towards the quadrupolar nucleus (Harris and Nesbitt 1988), even though optimum experimental conditions have already been explored for the case of ^{27}Al nuclei (Rocha et al. 1991; Kellberg et al. 1991; Morris and Ellis 1989; Mortis et al. 1990). Second, available and unequivocally assigned high-resolution ^{1}H MAS NMR spectra of the solid systems studied are required in order to correlate adequately the 2-D signals that appear in the spectra. Both requirements have recently been fulfilled by our group for the solid systems herewith analyzed (Alba et al. 2000, 2001a).

We hereby present the results of a systematic study of phyllosilicates by $^{1}H \rightarrow ^{27}Al$(2-D) CPMAS NMR spectroscopy. A method that provides resolution enhancement in ^{27}Al NMR spectra is reported, which allows a straightforward identification of aluminum in the same coordination but with different chemical environments. This work differs from the earliest ^{27}Al MAS NMR works on clays in the sense that, for the first time, spatial correlation between proton and aluminum has been established in clay minerals. Likewise, useful applications for such measurements are proposed in the last section of the manuscript.

Theoretical section

The quadrupolar double resonance experiment can be treated by analogy with the spin $I = 1/2$ case except for one condition; namely, the coherent adjustment of the matching pulse amplitude. The matching condition must be restated as: $\gamma^{[H]}.B_1{}^{[H]} = [I(I + 1) - m(m - 1)]^{1/2} \gamma^{[X]}.B_1{}^{[X]}$ (Hartmann and Hahn 1962); where $m \rightarrow (m\text{-}1)$ defines the transition considered. If a suitable "standard" compound is chosen such that the quadrupolar spin has a high-symmetric environment, the other transitions of the quadrupolar nucleus will be degenerated with the $+1/2 \rightarrow -1/2$ transition. For such a system it should be possible to observe cross polarization in a manner analogous to the spin-1/2 case (Harris and Nesbitt 1988).

In two-dimensional heteronuclear NMR correlation experiments, the $^{1}H \rightarrow ^{27}Al$ correlation is made through dipolar interactions. A variety of pulse sequences to implement this type of experiment were first introduced by Ernst and coworkers (Caravatti et al. 1982). The pulse sequence used in the present work is shown in Fig. 1a, where it is visualized in terms of four discrete time periods. The preparation period involves the relaxation of the proton reservoir towards thermal equilibrium. The frequency encoding of the protons occurs during the evolution period (t_1 domain), polarization transfer to aluminum during the mixing period and acquisition in the detection period. The Fourier transforms of the free-induction decays (FIDs) collected during the final period (t_2 domain) gave rise to a set of spectra which reflected the chemical shift and processes that occurred to the z magnetization during the mixing period. It was a second Fourier analysis, this one being

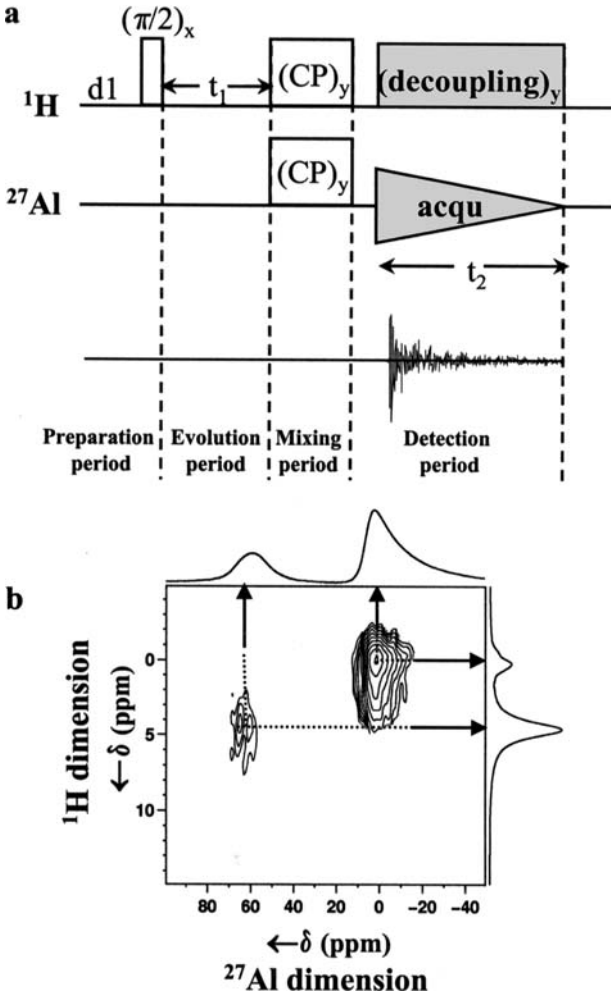

Fig. 1 **a** Pulse sequence used for the 2D ^{1}H-^{27}Al heteronuclear correlation NMR experiments. **b** Illustrative 2-D spectrum obtained by using this pulse sequence

in the t_1 domain, which finally gives the 2-D results that are presented below. An illustrative spectrum has been included in Fig. 1b.

Experimental

Materials selected

The samples examined in this study are 2:1 phyllosilicates, which consist of layers made up by the condensation of a central octahedral sheet and two tetrahedral sheets, one on each side as shown in Fig. 2. Individual tetrahedra are linked with three neighbouring tetrahedra to form a hexagonal pattern in the tetrahedral sheet. Octahedral compositions depend on the octahedral occupancy that can be either a full occupancy of the sheet if the cations are Mg^{2+} (trioctahedral minerals) or an occupancy of two-thirds of the available positions if the cations are Al^{3+} (dioctahedral minerals). The layers as described are electrically neutral but, in most cases, the isomorphous substitutions in the tetrahedral sheet, essentially Al^{3+} for Si^{4+}, and/or in the octahedral sheet confer a net negative charge to the layers that is balanced by hydrated interlayer cations.

In this structural arrangement, the aluminum can occupy three different positions in the network as summarized in Fig. 2:

1. Aluminum located in the tetrahedral sheet (Fig. 2a): aluminum atoms in tetrahedral coordination surrounded by three silicon tetrahedra (Al–O–Al linkages are forbidden) (Loewenstein 1954). The tetrahedra are arranged so that all their tips point in the same direction and the bases of all the tetrahedra are in the same plane, forming a hexagonal hole in contact with the interlayer space. The OH groups of the octahedra are located in the centre of the hexagonal cavities of the tetrahedral sheet, the orientation of the OH bond being different in the dioctahedral and trioctahedral smectites (Serratosa and Bradley 1958; Chatterjee et al. 2000; Madejová et al. 2000).
2. Aluminum located in the octahedral sheet (Fig. 2b): aluminum atoms are embedded in octahedral coordination, so that they are surrounded by four oxygen and two hydroxyls, which can occupy the two different relative positions represented in the figure.
3. Aluminum located in the interlayer space (Fig. 2c): hydrated aluminum is located in the interlayer space compensating for the net negative charge of the layer as an aquocomplex, $[Al(OH_2)_6]^{3+}$.

Samples of representative species among 2:1 phyllosilicates with compositions close to the ideal ones have been selected. All of them belong to the smectite group and include members of the dioctahedral and trioctahedral series with various tetrahedral Si/Al ratios and different interlayer compositions. The samples were supplied by the Source Clay Minerals Repository of Missouri University (Columbia). All the smectites selected are well-characterized materials, which have already been referenced (Alba et al. 2001b). The designation used hereafter of each sample is composed of two segments. The first one indicates the nature of the interlayer cation and the second segment the nature of the smectite (A for Arizona montmorillonite, L for laponite, B for beidellite, and S for saponite). Thus, Al–S signifies a saponite homoionized in Al^{3+}. A summary of the distribution of aluminum in the different structural sites for each sample studied is included in Fig. 3. This graph accounts for the amount of $Al^{[6]}$ in the octahedral sheet (x axis), $Al^{[4]}$ in the tetrahedral sheet (y axis) and $Al^{[6]}$ in the interlayer space (z axis). Those samples with a single aluminum environment, such as Na–S, Na–A or Al–L, are located along the axes and those with two different aluminum environments, Al–S and Na–A, are placed in the yz and xy planes, respectively. Note should be taken of the different scale for each axis, caused by the different amounts of aluminum allowed in each structural site. Thus, the maximum x value is ten times greater than the maximum z value and four times greater than the maximum y value. In consequence, the spectral sensitivity of aluminum in the octahedral sheet will be much higher than that of aluminum in the other structural sites.

Method

The MAS NMR experiments were performed on a Bruker DRX 400 spectrometer equipped with a multinuclear probe, operating at 400 and 104.2 MHz for ^{1}H and ^{27}Al, respectively. Powdered samples were packed into zirconia rotors and spun at 12 kHz. Apparent chemical shifts of nuclei were measured with respect to tetramethylsilane and $Al(H_2O)_6^{3+}$, for proton and aluminum,

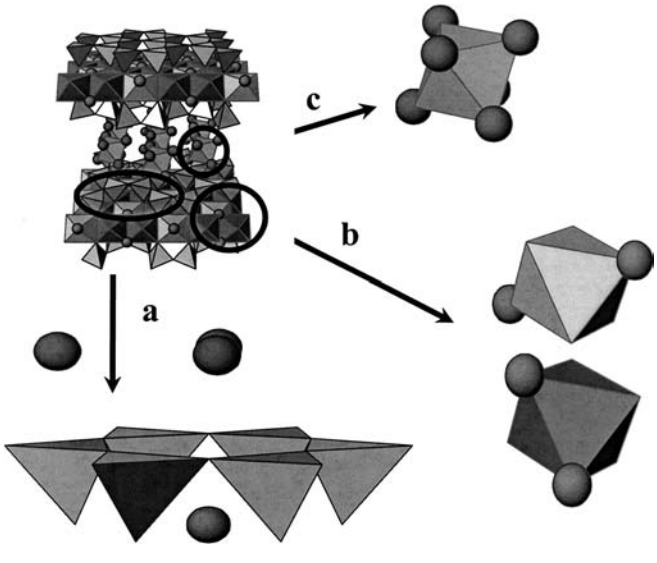

Fig. 2 a–c Diagram of aluminum location in 2:1 phyllosilicates. **a** view of pseudohexagonal hole of the tetrahedral sheet showing the location of tetrahedral aluminum. **b** Aluminums located in the octahedral sheet. **c** Aquocomplex of aluminum in the interlayer space

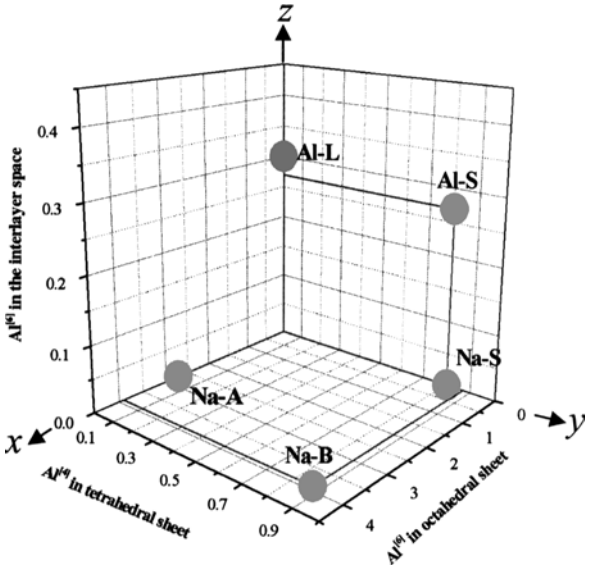

Fig. 3 3-D graph representing the distribution of aluminum ions in the samples examined. It displays the amount of aluminum in the octahedral (x axis) and the tetrahedral sheets (y axis) and in the interlayer space (z axis)

respectively. Adequate time intervals between successive accumulations were chosen in order to avoid saturation effects.

^{27}Al Bloch decays were recorded with very short radiofrequency pulses (0.9 μs, equivalent to $\pi/20$) and 100-ms recycle delays. ^{1}H MAS NMR spectra were obtained using typical $\pi/2$ pulse widths of 4.1 μs and a pulse spacing of 5 s.

^{1}H→^{27}Al cross-polarization experiments were performed under MAS and high-power proton decoupling, using a single contact. Spectra were acquired using a ^{1}H $\pi/2$ pulse of 4.8 μs, recycle delays of 250 ms, and optimized values of contact time between 100 μs and 1 ms. The criteria for the evaluation of a useful matching standard for quadrupolar nuclei are the same as those for spin-1/2 nuclei except for one additional constraint: the nuclear environment should have a high symmetry. As stated previously, this simplifies the transition contributions and essentially allows the nuclei to be treated in a fashion analogous to a spin-1/2 case. In this sense, a highly crystalline kaolinite was chosen as a potential ^{27}Al reference standard. In Fig. 4 the aluminum response to the cross-polarization experiment is shown. The spectrum is characterized by a sole aluminum environment which does not exhibit residual quadrupolar contributions in the MAS experiment as denoted by the lineshape of central transition ($+1/2 \rightarrow -1/2$) and by the small contribution of spinning sidebands, which have been marked with asterisks in Fig. 4. Thus, kaolinite is a suitable standard for calibrating the matching condition. A 12-kHz spinning speed was chosen because it is fast enough to remove almost all the spinning sideband contributions but small enough for the Hartmann–Hahn conditions to be met easily (see Fig. 4). Because only the central ($+1/2 \rightarrow -1/2$) transition is observed, excitation in the ^{1}H→^{27}Al CPMAS experiment is selective and therefore the Hartmann-Hahn condition is:

$$\gamma^{[H]} \cdot B_1{}^{[H]} = 3\gamma^{[Al]} \cdot B_1{}^{[Al]} \pm \text{n}.w_r \text{ (Meier 1992)},$$

being constant for all the experiments, since both the RF amplitude and the MAS speed were kept constant.

Two-dimensional ^{1}H→^{27}Al CPMAS spectra were obtained with the pulse sequence shown in Fig. 1. For each 2-D experiment a set of 80–120 FIDs was obtained with a t_1 increment of 5 μs and a dwell time of 5 μs. A squared sine line broadening was applied in both frequency domains.

Results and discussion

In this section, the results are presented as contour plots of the 2D ^{1}H →^{27}Al correlation experiments. The vertical axis represents the proton chemical shift scale and the horizontal axis the ^{27}Al chemical shift scale. In these two-dimensional ^{1}H→^{27}Al heteronuclear correlation spectra, the number of cross-peaks is related to the different aluminum sites in the sample and to the number of cross-polarization sources. The spectra above and at the sides of the 2-D graphs are the one-dimensional single-pulse spectra of ^{27}Al and ^{1}H, respectively. They are used to establish the connectivity. In order to separate clearly the two contributions of protons to the ^{1}H(SP) MAS NMR spectrum – structural hydroxyl group and water – two one-dimensional single pulse spectra are shown for the ^{1}H axis corresponding to the sample thoroughly hydrated (on the left) and once dehydrated (on the right). In those cases where the connectivity is not clear enough, this representation will be accompanied by an additional graph where the single pulse spectrum is compared with the corresponding projection of the cross-peak under discussion. The description of this second graph will be given in each particular case.

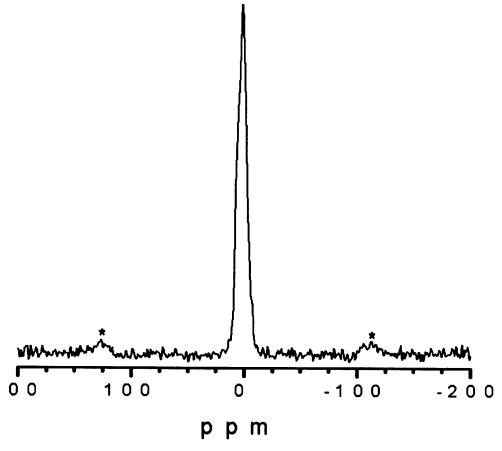

Fig. 4 ^{1}H-^{27}Al CPMAS NMR spectrum of kaolinite. The spinning side bands have been marked with asterisks

In general, the ^{1}H spectrum for a hydrated smectite consists of two peaks in the chemical shift ranges of 3–5 and 1.5–0.5 ppm. The peak at the lower field is attributed to water molecules and its position is sensitive to the nature of the interlayer cation. The peak at the higher field arises from protons of hydroxyl groups in the octahedral sheet, the exact position and line width of the signal being dependent on the nature of the smectite (Alba et al. 2003). Regarding the ^{27}Al spectrum, the 1-D aluminum signals are sensitive only to the coordination number of the aluminum atom in the AlO_n polyhedron. For tetrahedrally coordinated AlO_4 units in phyllosilicates, chemical shifts of about 60 to 70 ppm are observed, and octahedral AlO_6 groups resonate at −10 to 20 ppm (Sanz and Serratosa 1984; Lippmaa et al. 1986).

In a first step, spectra of a set of three smectites with a single aluminum environment are discussed in order to cover the three possible locations of this cation in the aluminosilicate framework (see Fig. 2). These samples are sodium-saturated saponite, Na-S, with Al^{3+} in the tetrahedral sheet; sodium-exchanged montmorillonite Arizona, Na–A, with aluminum in the octahedral sheet; and aluminum-exchanged laponite, Al–L, with Al^{3+} in the interlayer space (Fig. 3). Although laponite is a trioctahedral member without any framework aluminum, some minor aluminum environments are observed in ^{27}Al MAS NMR due to impurities, but they do not interfere in our study. This sample will be used to determine the polarization source of interlayer hexacoordinated aluminum.

Na-saponite, a trioctahedral smectite with an isomorphous substitution of Al for Si in the tetrahedral sheet, shows a ^{27}Al (SP) MAS NMR spectrum that is characterized by a single peak centred in the region of the tetrahedral coordination, as expected for this sample (see top of Fig. 5). Although two possible cross-polarization sources do exist for aluminum located in the tetrahedral sheet, interlayer water and structural hydroxyl groups, only a single cross-peak appears in the

2-D spectrum (see Fig. 5). The position of such a cross-peak correlates the aluminum signal at 65 ppm with the proton signal at 0.6 ppm. The polarization source is then unique and corresponds to protons of the hydroxyl group. Thus, it is clear that the hydroxyl site is the main source of cross-polarization, because of its relative rigidity and proximity to the tetrahedral aluminum atoms in comparison with interlayer water.

The ^{27}Al single-pulse spectrum of sodium-exchanged Arizona montmorillonite – a dioctahedral member with isomorphous substitution of Mg^{2+} for Al^{3+} in the octahedral sheet – has been included at the top of Fig. 6a. This spectrum exhibits a peak at ~0 ppm that is characteristic of AlO_6 units. Figure 6a also shows the 2-D spectrum with a single cross-peak centred at ~0 ppm in the aluminum domain (aluminum in octahedral coordination) and at ~2 ppm in the proton domain (structural hydroxyl). Since the dioctahedral smectites show a low resolution in the proton domain, the projections of the unique 2-D cross-peak in the aluminum dimension and in the proton dimension have been included in Fig. 6b and c, respectively. Regarding the ^{27}Al projection, this is similar to that obtained by aluminum single-pulse excitation (dashed line) and consists of a single signal at ~0 ppm that is assigned to the unique aluminum coordination in this smectite. In order to have a clear idea of the source of polarization, the 2-D proton projection (bottom spectrum in Fig. 6c) is compared with the single-pulse proton spectra obtained from the hydrated and dehydrated sample (solid and dashed line, respectively, top spectra in Fig. 6c). This graph shows that the unique cross-peak in the 2-D spectrum correlates the ^{27}Al signal at 0 ppm – Al[6], with the ^{1}H signal at 2 ppm – structural OH group. We therefore conclude that the cross-polarization of the ^{27}Al spins of the octahedral sheet of this smectite is originated only from structural hydroxyl groups.

Finally, laponite was chosen because it is a synthetic trioctahedral smectite with nominally no framework aluminum. However, the ^{27}Al(SP) MAS NMR spectrum of Na–L (plot at bottom of Fig. 7a) shows a peak in the chemical shift range of tetracoordinated aluminum, which can be due either to an impurity phase other than smectite or to the presence of aluminum traces in the tetrahedral sheet of smectite. The sample homoionized with aluminum, Al–L, shows a new contribution in the aluminum spectrum (plot at top of Fig. 7a) in the

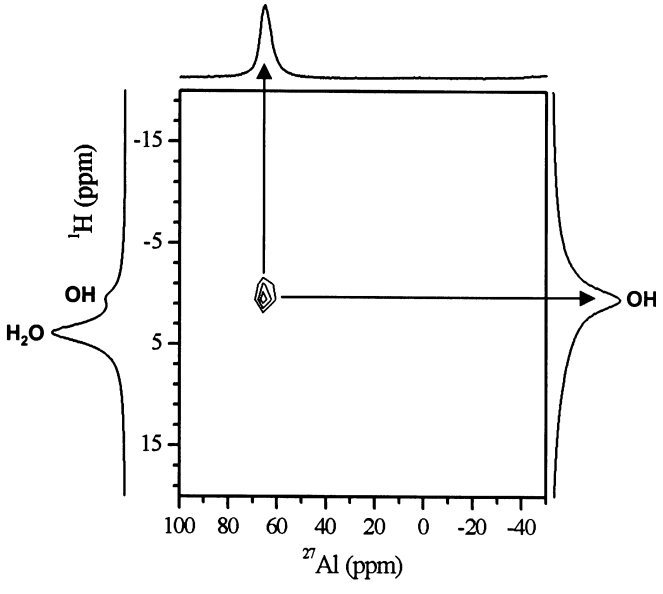

Fig. 5 Contour plot of the 2-D ^{1}H-^{27}Al correlation experiments of Na–S. The *vertical axis* represents the proton chemical shift scale and the *horizontal axis* the ^{27}Al chemical shift scale. The *spectra above and at the side of the figure* are the one-dimensional ^{27}Al and ^{1}H (SP) MAS NMR spectra, respectively

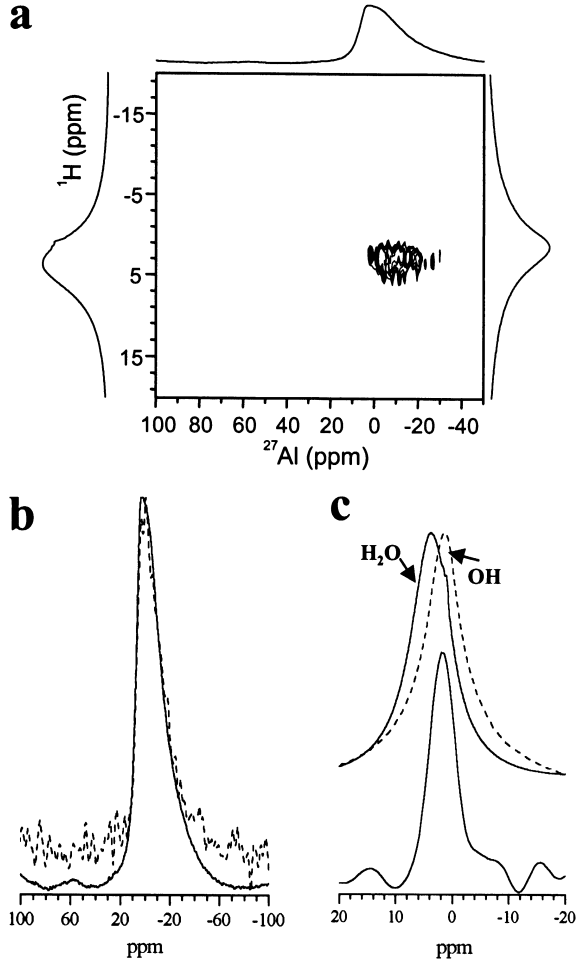

Fig. 6 **a** Contour plot of the 2-D ^{1}H-^{27}Al correlation experiments of Na–A. The *vertical axis* represents the proton chemical shift scale and the *horizontal axis* the ^{27}Al chemical shift scale. The *spectra above and at the side of the figure* are the one-dimensional ^{27}Al and ^{1}H (SP) MAS NMR spectra, respectively. **b** ^{27}Al spectra: the *solid line* corresponds to single-pulse excitation of the sample equilibrated at room temperature and the *dashed line* corresponds to the projection of the ^{1}H-^{27}Al(2D) CPMAS spectrum in the aluminum domain. **c** ^{1}H spectra: the plots at the *top of the figure* correspond to single-pulse excitation of the sample equilibrated at room temperature (*solid line*) and heated at 150 °C (*dashed line*), and the *plot at the bottom of the figure* corresponds to the projection of the ^{1}H-^{27}Al(2D) CPMAS spectrum in the proton domain

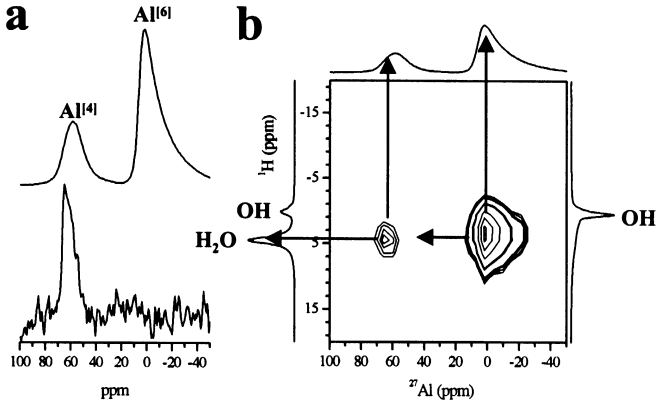

Fig. 7 a, b 2-D and 1-D ^{27}Al and ^{1}H MAS NMR spectra of Al–L. **a** ^{27}Al single-pulse excitation spectra of Na–L (*bottom*) and Al–L (*top*). **b** Contour plot of the 2-D ^{1}H-^{27}Al correlation experiments. The *vertical axis* represents the proton chemical shift scale and the *horizontal axis* the ^{27}Al chemical shift scale. The spectra *above and at the side of the figure* are the one-dimensional ^{27}Al and ^{1}H (SP) MAS NMR spectra, respectively

chemical shift range of hexacoordinated aluminum, as expected. The presence of two types of aluminum in Al–L has already been reported by Tennakoon et al. (1983, 1986). They proposed that the tetrahedral component results from either substitution of Al into a tetrahedral site within the clay framework during exchange or precipitation of a tetrahedral Al species during or subsequent to ion exchange. However, no direct evidence of the aluminum location was shown.

Fig. 8 a Contour plot of the 2-D ^{1}H-^{27}Al correlation experiments of Al–S. The *vertical axis* represents the proton chemical shift scale and the *horizontal axis* the ^{27}Al chemical shift scale. The spectra *above and at the side of the figure* are the one-dimensional ^{27}Al and ^{1}H (SP) MAS NMR spectra, respectively. **b** ^{1}H spectra: the plots *at the top of the figure* correspond to single-pulse excitation of the sample equilibrated at room temperature (*solid line*) and heated at 150 °C (*dashed line*) and the plots *at the bottom of the figure* correspond to the projection of both cross-peaks of the ^{1}H-^{27}Al (2D) CPMAS spectrum. The *solid line* represents the proton projection of octahedral aluminum and the *dashed line* represents the proton projection of tetrahedral aluminum

Figure 7b shows the correlation spectrum between aluminums and protons, a single cross-peak for each aluminum site being observed. This means that there is a single polarization source for each aluminum site. On one hand, there is no connectivity between structural hydroxyl groups and Al[4]; thus, it is clear that these minor contributions are not due to the substitution of Al into the tetrahedral sheet. On the other hand, the second cross-peak, Al[6], is correlated with the water signal expected for hydrated interlayer aluminum. Thus, the type of polarization source permits distinguishing of six-coordinated aluminum in the octahedral sheet – Al[6] correlated with structural hydroxyl – from that in the interlayer space – Al[6] correlated with water.

Once the sources of protons for each aluminum environment had been established, we then tried to differentiate signals when aluminum coexists in more than one structural site. For this purpose, a saponite sample, a smectite with aluminum in a tetrahedral site, was homoionized with Al^{3+}. The ^{27}Al (SP) MAS NMR spectrum, at the top of Fig. 8a, shows two peaks, one at ca. 60 ppm, assigned to four-coordinated aluminum, and one at 0 ppm assigned to six-coordinated aluminum. When the 2-D correlation experiment is performed, it is observed that each aluminum site has a single source of polarization (see Fig. 8a, in which there is one cross-peak for each aluminum environment). In order to identify the proton nature of these polarization sources, we have represented in Fig. 8b the proton projection of both cross-peaks (bottom of figure) and they are compared with the ^{1}H (SP) MAS NMR spectra (top of the figure) of the hydrated (solid line) and dehydrated (dashed line) samples. The tetrahedral aluminum (dashed line at bottom of Fig. 8b) is correlated with the proton signal at 0.6 ppm and the octahedral one (solid line at bottom of Fig. 8b) with the signal at 4.7 ppm. Thus, aluminum in the tetrahedral sheet is spatially correlated with the structural hydroxyl group and the exchangeable cation in the interlayer space is correlated with interlayer water species. Although the number of

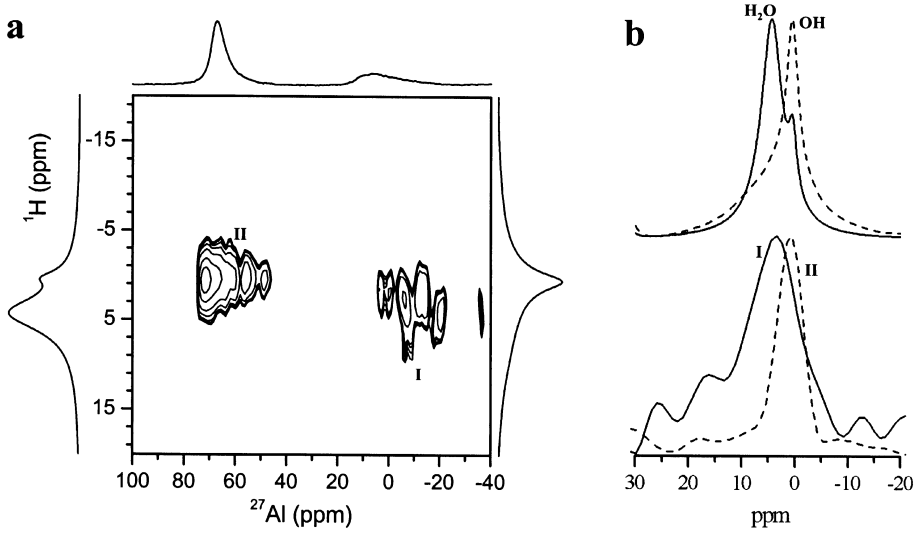

protons per aluminum is higher in aluminum nuclei located in the interlayer space than those located in the tetrahedral sheet, there is no increment in the intensity of the ^{27}Al (CP) signal of Al$^{[6]}$ vs. Al$^{[4]}$, the water proton mobility and the quadrupolar interactions of Al$^{[6]}$ being responsible for this fact.

A combination of aluminum in tetrahedral and octahedral sheets is found when sodium-exchanged beidellite, a dioctahedral member with isomorphous substitution of Al for Si in the tetrahedral sheet, is analyzed. Figure 9a shows the 2-D CPMAS NMR spectrum which exhibits two cross-peaks (the scale of the left one has been increased for a better observation) at aluminum chemical shifts of ca. 60 and 0 ppm, similar to the chemical shift values observed for Al–S. However, in this sample, Na–B, both aluminum nuclei are connected with hydroxyl groups (a comparison between proton projections of both signals is included at the bottom of Fig. 9b, and the single pulse-proton spectra of the hydrated and dehydrated samples are included at the top of the same figure). This means that both aluminum cations are occupying positions inside the aluminosilicate framework. Specifically, they are located in tetrahedral (Al$^{[4]}$) and octahedral sheets (Al$^{[6]}$) The intensity difference observed can be explained taking into account the following two facts: (1) Al$^{[6]}$/Al$^{[4]}$ ratio in this sample is about 4.5, and (2) the distance between the hydroxyl group and Al$^{[6]}$ is considerably shorter than the distance hydroxyl–Al$^{[4]}$, the efficiency of the magnetization transfer being inversely related to the distance between ^{1}H and ^{27}Al.

Once the correlation between different aluminum and proton sites has been well established, in a set of known smectite, an application of this methodology to an unknown material is included. Within the study of the interaction mechanisms between interlayer cations and smectites, we have recently described the formation of new crystalline phases of lutetium disilicate when lutetium-saturated smectites, or natural smectites in contact with lutetium ions in solution, are hydrothermally treated (Alba et al. 2001b). To understand the basis of the reaction mechanism involved, it is crucial to know the structural modifications of the remnant ions in the smectite after treatments. For this purpose, ^{1}H→^{27}Al(2D) CPMAS NMR has been applied to a saponite hydrothermally treated at 300 °C with a 3.5×10^{-3} M $Lu(NO_3)_3$ solution. Figure 10 shows the one-dimensional ^{27}Al and ^{1}H (SP) MAS NMR spectra and the contour plot of the 2D ^{1}H-^{27}Al correlation experiments. While the ^{27}Al single-pulse spectrum of the untreated saponite shows only one peak at ca. 60 ppm, assigned to four-coordinated aluminum (see the top of Fig. 5), the corresponding spectrum of the treated sample (see the top of Fig. 10) shows two signals, one at ca. 60 ppm and other weak peak at ca. 0 ppm, assigned to six-coordinated aluminum. In view of the single-pulse spectrum, one could contemplate two possibilities: (1) migration of aluminum from the tetrahedral sheet into the octahedral sheet, and/or, (2) migration of aluminum from the tetrahedral sheet into the interlayer space. The 2-D correlation experiment exhibits two cross-peaks, one for each aluminum environment. The aluminum

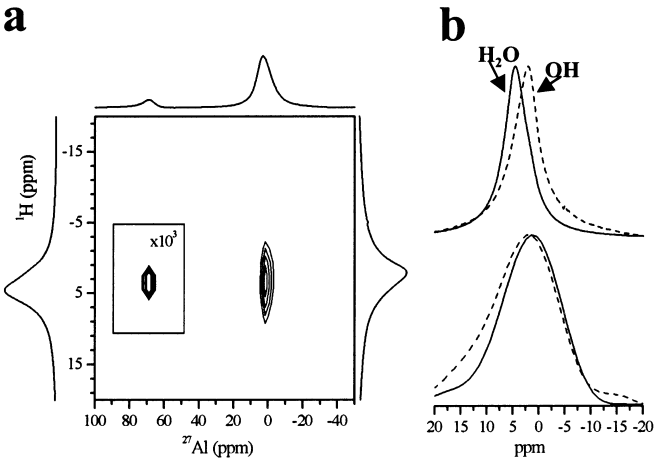

Fig. 9 2-D and 1-D ^{27}Al and ^{1}H MAS spectra of Na–B. **a** Contour plot of the 2-D ^{1}H-^{27}Al correlation experiment. The *vertical axis* represents the proton chemical shift scale and the *horizontal axis* the ^{27}Al chemical shift scale. The spectra *above and at the side of the figure* are the one-dimensional ^{27}Al and ^{1}H (SP) MAS NMR spectra respectively. **b** ^{1}H spectra: the plots *at the top of the figure* correspond to single-pulse excitation of the sample equilibrated at room temperature (*solid line*) and heated at 150 °C (*dashed line*) and the plots *at the bottom of the figure* correspond to the projection of both cross-peaks of the ^{1}H-^{27}Al(2D) CPMAS spectrum. The *solid line* represents the proton projection of octahedral aluminum and the *dashed line* represents the proton projection of tetrahedral aluminum

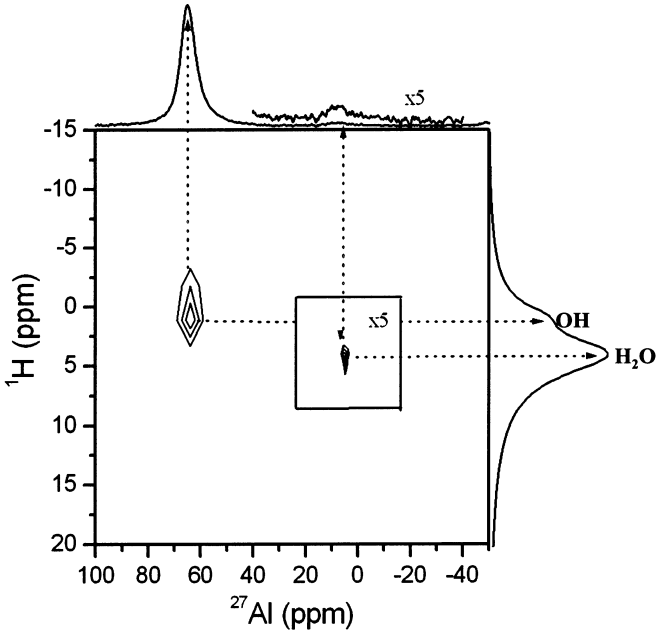

Fig. 10 Contour plot of the 2-D ^{1}H-^{27}Al correlation experiments of saponite treated at 300 °C for 48 h with a 3.5×10^{-3} M $Lu(NO_3)_3$ solution. The *vertical axis* represents the proton chemical shift scale and the *horizontal axis* the ^{27}Al chemical shift scale. The spectra *above and at the side of the figure* are the one-dimensional ^{27}Al and ^{1}H (SP) MAS NMR spectra, respectively

peak at ca. 60 ppm, $Al^{[4]}$, is correlated with the proton signal at 0.6 ppm (the signal corresponding to structural hydroxyl groups) and has an appearance similar to that observed for the untreated saponite. The aluminum peak at ca. 0 ppm, $Al^{[6]}$ is correlated with the proton signal at 4.7 ppm (signal corresponding to water) and it is not observed in the initial sample. In consequence, the hydrothermal treatment has caused a leaching of part of this framework aluminum into the interlayer space.

Concluding remarks

The combination of high-resolution MAS-NMR spectroscopy with a pulse sequence that allows the heteronuclear correlation between proton and aluminum to be established permitted us to distinguish not only aluminum with different coordination numbers but aluminum with different chemical environments. Moreover, this method offers a potential use in monitoring aluminum leaching that takes place in aluminosilicate reactions and in differentiating between framework and extraframework aluminum in other aluminosilicate-based materials, such as zeolites or mesoporous molecular sieves.

Acknowledgements We gratefully acknowledge financial support from the DGICYT (Project no. BQU2001–3138 and MAT2002–03504) and thank Dr. S. Steuernagel for his experimental assistance.

References

Alba MD, Becerro AI, Castro MA, Perdigón AC (2000) High-resolution H-1 MAS NMR spectra of 2:1 phyllosilicates. Chem Commun 37–38

Alba MD, Becerro AI, Castro MA, Perdigón AC (2001a) Two-dimensional heteronuclear H-1 <-> Al-27-correlated MAS NMR spectra of layered silicates. Chem Commun 249–250

Alba MD, Becerro AI, Castro MA, Perdigón AC (2001b) Hydrothermal reactivity of Lu-saturated smectites, part I. A long-range order study. Am Mineral 86: 115–123

Alba MD, Becerro AI, Castro MA, Perdigón AC, Trillo JM (2003) Inherent acidity of aqua metal ions in solids: an assay in layered aluminosilicates. J Phys Chem (B) 107: 3996–4001

Blumenfeld AL, Fripiat JJ (1997) Al-27-H-1 REDOR NMR and Al-27 spin-echo editing: a new way to characterize Bronsted and Lewis acidity in zeolites. J Phys Chem (B) 101: 6670–6675

Caravatti P, Bodenhausen G, Ernst RR (1982) Heteronuclear solid-state correlation spectroscopy. Chem Phys Lett 89: 363–367

Chatterjee A, Iwasaki T, Ebina T (2000) A novel method to correlate layer charge and the catalytic activity of 2:1 dioctahedral smectite clays in terms of binding the interlayer cation surrounded by monohydrate. J Phys Chem (A) 104: 8216–8223

Figueras F (1988) Pillared clays as catalysts. Catal Rev Sci Eng 30: 457–499

Harris RK, Nesbitt GJ (1988) Cross-polarization for quadrupolar nuclei proton to Na-23. J Magn Reson 78: 245–256

Hartmann SR, Hahn EL (1962) Nuclear double resonance in rotating frame. Phys Rev 128: 2042

Kellberg L, Linsten M, Jakobsen HJ (1991) Al-27(H-1) Cross-polarization and ultrahigh-speed Al-27 Mas NMR spectroscopy in the characterization of Usy zeolites. Chem Phys Lett 182: 120–126

Kirkpatrick RJ, Smith KA, Schramm S, Turner G, Yang WH (1985) Solid-state nuclear magnetic-resonance spectroscopy of minerals. Ann Rev Earth Planet Sci 13: 29–47

Lippmaa E, Samoson A, Mägi M (1986) High-resolution Al-27 NMR of aluminosilicates. J Am Chem Soc 108: 1730–1735

Loewenstein W (1954) The distribution of aluminum in the tetrahedra of silicates and aluminates. Am Mineral 39: 92–96

Madejova J, Bujdak J, Petit S, Komadel P (2000) Effects of chemical composition and temperature of heating on the infrared spectra of Li-saturated dioctahedral smectites. (I) Mid-infrared region. Clay Miner 35: 739–751

Meadows MD, Smith KA, Kinsey RA, Rothgeb TM, Skarjune RP, Oldfield E (1982) High-resolution solid-state NMR of quadrupolar nuclei. Proceedings National Academy of Sciences USA. Phy Sci 79: 1351–1355

Meier BH (1992) Cross-polarization under fast magic-angle spinning: thermodynamical considerations. Chem Phys Lett 88: 201–207

Mitchell IV (1990) Pillared layered structures. Elsevier, Amsterdam

Mokaya R, Jones W, Luan ZH, Alba MD, Klinowski J (1996) Acidity and catalytic activity of the mesoporous aluminosilicate molecular sieve MCM-41 Catal Lett 37: 113–120

Morris HD, Ellis PD (1989) Al-27 cross-polarization of aluminas – the NMR-spectroscopy of surface aluminum atoms. J Am Chem Soc 111: 6045–6049

Morris HD, Bank S, Ellis PD (1990) Al-27 NMR-spectroscopy of iron-bearing montmorillonite clays. J Phys Chem 94: 3121–3129

Muller D, Gessner W, Behrens HJ, Scheler G (1981) Determination of the aluminum coordination in aluminum–oxygen compounds by solid-state high-resolution Al-27 NMR. Chem Phys Lett 79: 59–62

Oldfield E, Kirkpatrick RJ (1985) High-resolution nuclear magnetic-resonance of inorganic solids science 227: 1537–1544

Ray GJ, Meyers BL, Marshall CL (1987) Si-29 and Al-27 NMR-study of steamed faujasites – evidence for nonframework tetrahedrally bound aluminum. Zeolites 7: 307–310

Rocha J, Klinowski J (1991) Al-27 solid-state NMR-spectra of ultrastable zeolite-Y with fast magic-angle spinning and H-1-Al-27 cross-polarization J Chem Soc Chem Commun 1121–1122

Sanz J, Serratosa JM (1984) Si-29 and Al-27 high-resolution MAS-NMR spectra of phyllosilicates J Am Chem Soc 106: 4790–4796

Serratosa JM, Bradley WF (1958) Determination of the orientation of OH bond axes in layer silicates by infrared absorption. J Phys Chem 62: 1164–1167

Tennakoon DTB, Schlögl R, Rayment T, Klinowski J, Jones W, Thomas JM (1983) The characterization of clay organic systems. Clay Miner. 18: 357–371

Tennakoon DTB, Thomas JM, Jones W, Carpenter TA, Ramdas S (1986) Characterization of clays and clay organic-systems – cation diffusion and dehydroxylation. J Chem Soc Faraday Trans 1 82: 545–562

Vega A (1992) Solid-state Nucl Magn Reson 1: 17

Weisz PB, Frilette VJ (1960) Intracrystalline and molecular-shape-selective catalysis by zeolite salts. J Phys Chem 64: 382–382

Yingcai L, Mingyang J, Yaojun S, Tailiu W, Liping W, Lun F (1996) J Chem Soc Faraday Trans 92: 1647